Influence of dielectric nanoparticles addition on electroconductivity and other properties of carbon nanotubes-based acrylic coatings

Szymon Kugler, Krzysztof Kowalczyk*, Tadeusz Spychaj
West Pomeranian University of Technology in Szczecin (WPUT), Polymer Institute, Pulaskiego 10, 70-322 Szczecin, Poland
*Corresponding author. Tel. +48 91 449 4178; fax: +48 91 449 4247. E-mail: kkowalczyk@zut.edu.pl

Abstract

The coating compositions based on commercial acrylic aqueous dispersion and carbon nanotubes (CNT) were modified with dielectric inorganic oxide nanoparticles (DNP), i.e. alumina, silica or titania. The influence of DNP type and content (0, 20 or 50 wt.%) on electrical, optical, mechanical and thermal features of the coatings has been investigated. The samples containing silica reached significantly lower electrical surface resistivity and higher transparency (e.g. $3.6 \cdot 10^7$ Ω and 70%, respectively for the material containing 0.25 wt.% of CNT and 50 wt.% of silica) than the reference sample (with CNT only) as well as the samples with similar CNT and other DNP (alumina or titania) content. Moreover, the samples containing 1 wt.% of CNT and 50 wt.% of silica or titania nanoparticles exhibited higher hardness (ca. 300% increment) and lower gloss (reduction from 80 G.U. to 48 G.U. and 0.3 G.U., respectively) in relation to the sample with CNT only. Additionally, the presence of CNT and DNP resulted in thermal stability increase of acrylic coatings up to 12 °C (for the samples filled with alumina or silica).

Keywords: Surface resistivity; Electroconductive coatings; Carbon nanotubes; Silica; Titania; Alumina

1. Introduction

The nanocomposite polymer films and coatings based on carbon nanotubes (CNT) are the subjects of growing attention due to their easy modification of electrical, thermal, and mechanical features. The addition of CNT markedly reduces electrical surface [1-4] or bulk resistivity [5-7] as well as improves storage modulus [7], tensile strength [4,8], corrosion resistance [6,9], tribological properties [10], hydrophobicity [2], thermal stability [11] and change glass transition temperature (T_g) [4] of polymer layers. Nevertheless, the modification of film-forming compositions with CNT reduces their optical transparency [1,2]. Polymeric binders used for nanocomposites preparation based on acrylates [1], epoxy resins [3,5,9], polyesters [8,12] or poly(ethylene oxide) [10]. These systems can be applied onto a substrate by casting [1,4,5,7], doctor blade/knife coating [8], spray coating [2,11], spin coating [3,10,12] or roll-blade casting [9] methods. The most compositions with CNT contained solvents [2,4,7,9-12]; only a few papers described UV-curable [1], two-component solventless [3,5] or one-component water-borne compositions [6,13,14]. Generally, the mentioned systems were filled with multi-walled CNT [1-11]; only a few articles reported using single-walled CNT [12]. The majority of described compositions were based on laboratory-made binders and/or CNT [2,4,6,7,10,12], and commercially available components were seldomly applied [1,3,8].

It is known that the presence of non-conductive solid particles resulted in electrical conductivity increase of bulk polymer nanocomposites with CNT [15-23], however, some announcements of the opposite effect (i.e. conductivity reduction) have been reported as well [24,25]. Generally, that phenomenon is explained as volume exclusion effect of non-conductive phase in the nanocomposite system [15,16,20-22]. Furthermore, mentioned dielectric phase can also improve thermal or mechanical features of materials filled with CNT [16,18,26].

Despite the potential benefits of additional dielectric phase presence in a nanocomposite, there is no report on films/coatings modified with CNT and auxiliary dielectric nanoparticles. The aim of this work was to investigate the acrylic coatings filled with CNT and dielectric inorganic oxide nanoparticles (DNP). The water-borne film-forming system was chosen to meet the environmental protection requirements for volatile organic compounds emission. Commercially available components (i.e. CNT, acrylic resin and DNP aqueous dispersions) facilitate application of prepared materials on a large scale.

2. Experimental

2.1. Materials

The following materials were used:

- commercial aqueous dispersion of methyl methacrylate, 2-ethylhexyl acrylate and styrene copolymer, 50 wt.% of solids, viscosity 250 mPa·s, glass transition temperatures -10 °C (shell of copolymer particle) and 50 °C (core), minimum film formation temperature 1 °C, average particle diameter 100 nm (Mowilith LDM 7411, Celanese Emulsions GmbH, Germany);
- aqueous dispersion of commercial multi-walled carbon nanotubes NC7000 (2 wt.% of MWCNT), with average length 1.5 μm, average diameter 9.5 nm, and average specific surface 275 m^2 g^{-1} (Nanocyl, Belgium); dispersion was prepared in WPUT (Szczecin) laboratory via sonication;
- commercial aqueous dispersion of alumina, 50 wt.% of Al_2O_3 with average diameter 40 nm and density 3.9 g cm^{-3} (NanoByk 3600, Byk-Chemie, Germany);
- commercial aqueous dispersion of silica, 40 wt.% of SiO_2 with average diameter 18 nm and density 2.2 g cm^{-3} (Binzil CC40, AkzoNobel, The Netherlands);
- aqueous dispersion (20 wt.% of solids) of commercial TiO_2 nanopowder with average diameter 25 nm and density 4.2 g cm^{-3} (P25, Evonik, Germany); dispersion was prepared via sonication;
- commercial auxiliary silicone additive for aqueous coating systems (BYK-094, BYK-Chemie, Germany).

2.2. Sample preparation

The acrylic coating compositions with CNT, DNP (i.e. Al_2O_3, SiO_2 or TiO_2) and BYK-094 (0.5 wt.%) were prepared according to the scheme presented in Supplement 1. They were applied onto glass and poly(ethylene terephthalate) (PET) substrates using a gap applicator and dried for 24 h at room temperature. The coatings (thickness of 50±2 μm) were abbreviated to N-C*x* (systems with CNT), N-C*x*/A*y* (CNT and Al_2O_3), N-C*x*/S*y* (CNT and SiO_2) and N-C*x*/T*y* (CNT and TiO_2), where *x* and *y* mean CNT and DNP content (wt.%) in a dry film, respectively (as in Table 1).

2.3. Methods

The electrical surface resistivity of prepared nanocomposites (glass substrate, 20 °C, 50% of RH, 10 V) was determined using 6517A electrometer with electrode set (8009, Keithley, USA). Transmission electron microscopy analysis was performed using JEM 1200EX microscope (Jeol, Japan). The coatings transparency on a PET foil was measured by UV-Vis spectrophotometer (V-630; Jasco, USA). The pendulum hardness of coatings (glass substrate, PN-EN ISO 1522 standard) was tested by means of König pendulum (AWS-5; Dozafil, Poland). The surface roughness (R_z parameter) was assessed using laser scanning microscope VK-9700 (Keyence, USA). The zeta potential values of the acrylic copolymer, DNP and CNT aqueous dispersions were measured using Zetasizer Nano ZS (Malvern, UK). The surface of the samples was analyzed using Fourier-transform infrared spectroscopy (Nexus; Thermo Nicolet, USA).

Gloss at 20° was determined using Rhopoint IQ206085 (Rhopoint Instruments, UK) in compliance with the ISO 2813 standard. The coatings adhesion to a glass substrate (cross-cut

method, PN-EN ISO 2409) was tested as well. Glass transition temperature (T_g) of the nanocomposites was evaluated by differential scanning calorimetry (DSC) and dynamic mechanical analysis (DMA). DSC tests were performed in a range of -20 – 180 °C (heating rate of 5 °C/min) by means of Q100 calorimeter (TA Instruments, USA). DMA tests were made in the following conditions: tension test in a range of 0 – 140 °C, heating rate of 3 °C/min, 1 Hz of frequency, amplitude 15 μm (DMA Q800; TA Instruments); the T_g values on a basis of tan delta peak were determined. Thermogravimetric analysis (TGA) was carried out using Q5000 thermoanalyzer (TA Instruments); temperature range was 20–600 °C with heating rate of 10 °C/min (air atmosphere).

3. Results and discussion

As it can be seen in Table 1, addition of non-conductive DNP markedly influenced electrical surface resistivity of CNT-based acrylic coatings. The values of that parameter for the samples containing 50 wt.% of DNP (alumina, silica or titania) are shown in Fig. 1. Generally, surface resistivity of the coatings depends on DNP type and CNT content. According to the reference data [27] the analyzed samples may be divided into three categories: insulating material (surface resistivity $>10^{11}$ Ω), static dissipative material (10^5–10^{11} Ω) and conductive material ($<10^5$ Ω). The static dissipative characteristic was reached for the samples containing CNT in the amount of: 0.7 wt.% (reference material without DNP, N-C0.7), 0.6 wt.% (sample with alumina, N-C0.6/A50), 0.5 wt.% (sample with titania, N-C0.5/T50) and 0.25 wt.% (sample with silica, N-C0.25/S50). Moreover, addition of DNP allowed to obtain electroconductive films at 2 wt.% content of CNT; surface resistivity for these samples was more than one order of magnitude lower in relation to the reference sample with CNT only (N-C2, Fig. 1). This phenomenon may be explained by excluded volume effect in CNT-modified matrix containing non-conductive nanoparticles. That effect was observed in bulk nanocomposites with CNT [15,16,20-22], but no paper describing influence of DNP on electrical properties of thin films containing carbon nanofillers is available. Fig. 2 shows a simplified scheme of the mentioned phenomenon. In Fig. 2A the CNT content in a polymeric matrix was too low to cause electrical percolation. When DNP was added partially replacing polymer matrix (the new phase entirely impermeable for CNT nanoparticles) (Fig. 2B), CNT concentration in the organic phase increased and the carbon nanofiller created conductive paths enabling current flow (CNT content in the coating without DNP and coating with DNP were the same). Taking into consideration the excluded volume effect, it could be noted that CNT content in the organic phase is crucial for electroconductive properties of the material. Therefore, surface resistivity values for acrylic coatings as a function of CNT concentration in the organic phase (i.e. data for samples with 1 wt.% of CNT and various DNP content) are presented in Fig. 3. It can be seen that surface resistivity of the nanocomposites containing CNT and DNP was distinctly lower than the values recorded for the reference samples with the same CNT content in the acrylic phase (N-C samples). Nevertheless, in the case of DNP-modified films (N-C1/DNP-type), the analyzed electrical property did not generally depend on the type and size of dielectric nanoparticles. On the other hand, the samples with 50 wt.% of DNP and <1 wt.% of CNT (concentration in the dry coating) exhibited different surface resistivity values and percolation thresholds were affected by the type of inorganic particles, i.e. SiO_2-modified coatings showed considerably lower values of these parameters than samples with Al_2O_3 or TiO_2 (Fig. 1). In the literature the influence of DNP type on electrical properties of bulk CNT-based nanocomposites is explained: (i) hydrophilic silica exhibits lower affinity for aromatic structure of CNT than titania [28], (ii) titania creates agglomerates with CNT which interrupt connections in CNT network [29], (iii) the presence of silica causes forming tiny CNT agglomerates which improves electroconductive properties [30] and (iv) alumina nanoparticles may act as dielectric obstacles for CNT [26]. Probably, these theories are not fully suitable for presented

coating systems because these compositions were formed using low viscous, polymeric aqueous dispersion as well as the content of DNP was markedly higher (up to 50 wt.%) in comparison to the materials described in [26,28-30].

In order to explain different percolation thresholds phenomenon for the samples with alumina and silica (Fig. 1), their surfaces (FT-IR spectroscopy) and roughness were investigated. It was discovered that IR spectra of the sample without DNP (N-C0) and sample containing 50 wt.% of alumina (N-C0/A50) were similar; mainly peaks at 2950, 1780, 1500 and 1200 cm^{-1} corresponding to acrylic matrix were observed (Fig. 4A). On the other hand, the IR spectrum of film modified with 50 wt.% of silica (N-C0/S50) was characterized by significant reduction of mentioned peaks and additional peak at 1050 cm^{-1}, i.e. characteristic band for SiO_2 (Fig. 4B) has been noted. Thus, large amount of silica was present on N-C0/S50 surface, in contrast to alumina, which generally was not detected on N-C0/A50 sample surface.

This conclusion was confirmed by the surface roughness analysis. The R_z parameter values for unfilled sample (N-C0) and coating with alumina (N-C0/A50) were similar (0.39 and 0.2 μm, respectively), whereas R_z for silica-modified material was significantly higher (1.69 μm) than for the reference sample. Thus, silica was probably located on the surface of a dry coating while alumina sedimented during drying of the water-borne composition.

Sedimented Al_2O_3 particles in the composite was observed on TEM images of sample cross-sections as well (Fig. 5A, Supplement 2A). Inhomogeneity of the polymer layer with alumina was probably caused by limited stability of Al_2O_3 aqueous dispersion. Zeta potential value for that system was low and positive (i.e. +9.4 mV) while it is known that 30 mV is a threshold for a dispersion stability. Sedimentation of DNP in a film was also observed for N-C1/T50 sample containing TiO_2 (but not so noticeable as for the sample with Al_2O_3) (Fig. 5C, Supplement 2C). Although zeta potential of titania aqueous dispersion reached -29.1 mV, the mentioned phenomenon was probably affected by extremely high density of that nanofiller (4.2 g/cm^3) in relation to alumina (3.9 g/cm^3) and especially to silica (2.2 g/cm^3).

Generally, considering the densities of the DNP as well as zeta potential values for the aqueous dispersions of alumina (+9.4 mV), titania (-29.1 mV), silica (-29.4 mV), CNT (-58.2 mV) and acrylic binder (-53.7 mV), it could be claimed the coating compositions based on CNT and silica (N-C/S systems) should be more stable during storage, application and drying than the others. Moreover, due to relatively low density of SiO_2, volumetric content of acrylic phase in the nanocomposites with silica was lower than in comparable samples containing alumina or titania. In fact, uniform dissipation of SiO_2 in the dry coating was noted (Fig. 5B, Supplement 2B). Thus, higher electrical conductivity of the N-C/S samples (in comparison with N-C/A and N-C/T; Fig. 1) was caused by stronger excluded volume effect. In other words, low volumetric content of polymeric matrix in the upper part of the sample containing silica (i.e. high volumetric content of DNP totally impermeable for CNT) significantly reduced surface resistivity in comparison to the samples with settled DNP. It is noteworthy that TEM analysis of the silica-modified composite revealed a large amount of CNT protruding from the film surface (Fig. 5B, Supplement 2B). Probably, during drying process of the composition with high DNP volume concentration, relatively stiff CNT were ejected from the film. Additionally, flotation of some porous silica particles enhanced that process. The presence of carbon nanotubes on the coating surface might be the main reason of higher surface electrical conductivity of N-C/S-type samples (Fig. 1). This phenomenon was not observed for the samples filled with alumina or titania where carbon nanofiller was entirely located in the polymeric phase (i.e. in coalesced shells of polymer particles) among DNP.

It should be noted that materials containing CNT and silica showed significantly higher electrical conductivity in comparison with the reported coatings based on solvent-borne [2], water-borne [13,14] and solventless coating compositions without DNP [5]. Only UV-cured

layers [1] exhibited higher surface conductivity than N-C/S samples with 50 wt.% of silica. Graphical comparison of these systems is shown in Fig. 6.

The addition of DNP into water-borne acrylic coating compositions can significantly affect hardness of dry coatings. In the case of systems containing 1 wt.% of CNT (Fig. 7A), silica and titania particles distinctly increased hardness of the materials (from 27 to ca. 90 hardness units), whereas alumina did not influence the discussed feature. Fig. 7B presents the enhancement of the films hardness in relation to CNT content. Generally, it can be observed that: (i) CNT improved hardness of unfilled samples and samples with DNP; (ii) the addition of the lowest CNT amount into systems containing silica or titania caused significant increase of their hardness. Despite this, the alumina-modified samples reached the lowest values of this parameter. It was probably affected by Al_2O_3 settling phenomenon during coating drying process (this fact was confirmed by the results of TEM images analysis of N-C1/A50 sample; Fig. 5A). In that case, concentration of hard inorganic particles near the coating surface was significantly reduced in comparison to similar samples containing silica or titania.

The described behavior of DNP also influenced gloss of the obtained films (Table 1). It can be observed that analyzed parameter depended mainly on a type of DNP incorporated but not on its dose. The samples modified with alumina exhibited markedly higher gloss (e.g. 111 G.U. for N-C0/A50) than the samples with silica (65 G.U. for N-C0/S50). It was caused by a settling of the former nanofiller during film formation. Interestingly, titania modified samples showed extremely low gloss (1 G.U. for N-C0/T50) as well as low transparency values in relation to similar samples with other type of DNP (Table 1). Although the transparency reduction noted for the layers with TiO_2 was caused by a high refractive index value of that nanofiller, low gloss of these samples was related to the high surface roughness (R_z=2.97 μm). TEM images of coating containing CNT and titania (Fig. 5C, Supplement 2C) showed polymer-rich and titania-rich areas in the sample. Probably, during film drying process the mentioned material inhomogeneity (areas characterized by different DNP volume concentration values) affected surface roughness and its gloss.

Considering CNT content in films filled with DNP, it should be noted that concentration of that nanofiller did not significantly reduce gloss of the samples. In the case of silica-filled systems, their gloss decreased only from 65 G.U. (N-C0/S50) to 48 G.U. (the sample with 1 wt.% of CNT; N-C1/S50). It means, that the considerable amount of CNT was located inside the coating (not on its surface). On the other hand, it caused markedly diminution of film transparency (Table 1, Supplement 3). The CNT behaved like a black pigment strongly reducing that optical feature. As mentioned above, the lowest transparency was registered for the samples with titania (white pigment) showing higher refractive index (2.7) in comparison with acrylic matrix (ca. 1.5) and other DNP types (1.5 for SiO_2 and 1.6 for Al_2O_3) [31].

As it can be seen in Table 1, the reference sample with 1 wt.% of CNT (N-C1) exhibited 14% transparency, while DNP-based material with similar surface resistivity (sample with silica; N-C0.25/S50) reached unusually high transparency (70%). Taking into consideration systems (presented in a literature) with similar surface resistivity and thickness values to N-C0.25/S50, it can be observed that transparency of the sample (0.25 wt.% of CNT and 50 wt.% of SiO_2) was almost the same as for solventless coatings with a significantly lower CNT content (i.e. 0.1 wt.%) [1] as well as noticeably higher than for solvent-borne material containing 7 wt.% of CNT [2]. It demonstrates that transparency of CNT-filled coatings can be effectively enhanced by DNP addition.

Generally, modification of CNT-filled compositions with DNP reduced adhesion of dry coatings to a glass substrate (Table 1). The value of this parameter decreased from 0 ° (reference films without or with CNT) to 1 ° (N-C0/T50), 2 ° (N-C0/A50) and 3 ° (N-C0/S50). Fortunately, the presence of carbon nanofiller in DNP-filled materials reverted this trend; the samples with CNT and DNP achieved noticeably higher adhesion than the materials

containing DNP only. Weaker adherence of the samples with DNP was caused by low polymeric binder content in a dry layer. Negative influence of high PVC (i.e. pigment/filler volume concentration) value on substrate wetting and coatings adhesion was observed and described by many authors, e.g. [32,33]. On the other hand, CNT positively affected mechanical adhesion of coatings to a glass substrate due to high aspect ratio (i.e. L/D ratio) of that nanofiller [34,35]. Additionally, elongated shape of the carbon nanofiller might limit DNP sedimentation during film formation. In that case, an increment of PVC value in a lower part of a coating is insignificant. For example, the addition of 0.5 wt.% of CNT upgrades coatings adhesion from 2 ° (N-C0/A50) to 1 ° (N-C0.5/A50).

Glass transition temperature (T_g) values of the coatings evaluated by DSC and DMA techniques are presented in Table 1. Additionally, DSC curves are shown in Supplement 4. In general, the modification of coatings with CNT negligible changed T_g of polymeric binder; it correlates with the literature data for CNT-modified layers [13,14]. It should be noted that the T_g values (DSC) of the reference sample (N-C0) were ca. -10 °C (core of acrylic particle) and 51 °C (shell) and corresponded with these declared by the binder manufacturer (-10 and -50 °C). Interestingly, the addition of some DNP reduced T_g of the core (alumina, titania) and the shell (alumina) of acrylic particles. In the case of materials containing 20 wt.% or 50 wt.% of TiO_2, T_g of the core decreased to -12.8 °C (samples with and without CNT). A significant variation of T_g (in relation to CNT or DNP content) was not recorded for dry films using DMA technique. It should be noted that the differences between T_g values determined by that two methods resulted from different features measured by the techniques, i.e. change of mechanical properties (DMA) or specific heat (DSC). Nevertheless, Tg value of polymeric particles core did not increase by CNT and/or DNP addition, thus coalescence process (during film formation) probably was not disturbed. Indeed, uncoalesced polymeric grains were not observed in TEM images of the samples with nanofillers (Fig. 5). High transparency of the sample containing 50 wt.% of SiO_2 (84%, N-C0/S50, Tab. 1) was caused by similar refractive index values of silica and the binder as well as by high homogeneity of the formed films. Influence of CNT on polymeric dispersion coalescence was investigated in [36].

Influence of CNT and DNP on thermal stability (determined by TGA technique) of the prepared coatings is shown in Fig. 8 (and in Supplement 5). The thermal stability is expressed as T_{10} temperature, i.e. temperature of 10% mass loss. Fig. 8A presents T_{10} temperatures for materials with DNP (without CNT); T_{10} reduction for most investigated samples was observed. For the materials containing 50 wt.% of DNP, T_{10} decreased from 326 °C (N-C0) to 320 °C (samples with titania; N-C0/T50), 304 °C (alumina; N-C0/A50) and 302 °C (silica; N-C0/S50), respectively. On the other hand, the CNT-based samples (with or without 50 wt.% of DNP), exhibited significantly higher thermal stability in relation to the reference system (without CNT and DNP; N-C0) (Fig. 8B). Introduction 1 wt.% of CNT resulted in T_{10} parameter increase from 326 °C (N-C0) up to ca. 338 °C (N-C1, N-C1/A50, N-C1/S50). Among the systems containing CNT and DNP nanoparticles, these with alumina showed the most pronounced increment of thermal stability, which was in accordance with the literature data [26].

4. Conclusions

The properties of water-borne acrylic coating compositions and coatings containing carbon nanotubes and significant amount of dielectric inorganic oxide nanofillers (DNP) have been described for the first time in a literature. The addition of DNP allowed to diminish the carbon nanofiller content in films maintaining appropriate electrical surface resistivity owing to excluded volume effect. Reduced CNT concentration in the coatings (at the constant concentration of that nanofiller in acrylic matrix) enabled to obtain systems with high transparency; that phenomenon was particularly observed for silica-filled nanocomposite coatings. Moreover, the presence of CNT/DNP mixture in acrylic films resulted in their

hardness enhancement (except for the system modified with alumina due to its sedimentation during film formation process). This effect was confirmed by surface roughness measurements, FTIR as well as zeta potential analyzes. Additionally, it was revealed that CNT addition improved adhesion (to a glass substrate) and thermal stability of DNP-modified samples. Generally, it could be concluded that investigated properties of prepared materials (i.e. electrical surface resistivity, hardness, transparency, gloss, adhesion, and thermal stability) depend on CNT presence as well as DNP type and content in the system. It seemed that the most optimal features of acrylic coatings were achieved using CNT (0.25 wt.%) and silica (50 wt.%). Due to relatively low electrical surface resistivity ($<10^{11}$ Ω) and accepted mechanical as well as thermal features, the coatings could be applied as static charge dissipative layers [2,13,27,37], e.g. protective top coatings for machineries and equipment used in explosive zones. Moreover, their relatively high light transmittance allows to apply them onto transparent substrates (e.g. lampshades in mines, sight-glasses in chemical installations). According to [37,38] prepared coating systems (with the lowest surface resistivity) could also be utilized as electromagnetic interference (EMI) shields fulfilling the requirements for such compositions (adequate conductive features and easy application onto sophisticatedly shaped surface). Nevertheless, the crucial parameter for EMI shielding efficiency is volume resistivity of a covering material [39,40]. The relations between electrical surface resistivity and bulk resistivity have already be described in the literature [4,5], however they concerned homogeneous materials only. Thus, influence of DNP on electrical volume resistivity as well as on EMI shielding efficiency of the CNT-filled acrylic coatings is going to be thoroughly investigated.

Acknowledgments

This work was financially supported by Polish National Science Centre (project no. 2014/13/N/ST8/00092: “Electroconductive polymeric coatings containing carbon nanofillers and dielectric domains”).

Authors thank Celanese Emulsions GmbH and Byk-Chemie GmbH for supplying the components of coating compositions and Ms. Katarzyna Wilpiszewska (West Pomeranian University of Technology in Szczecin) for polymer layers roughness analysis.

Literature

[1] H. Ha, S.C. Kim, K. Ha, UV curing kinetics and properties of polyurethane acrylate/multi-walled carbon nanotube coatings, Macromol. Res. 18 (2010) 674–679. doi:10.1007/s13233-010-0705-8.

[2] J. Liu, R. Liu, Y. Yuan, S. Zhang, X. Liu, Preparation of superhydrophobic antistatic coatings from branched alternating copolymers P(St-alt-MAn) and carbon nanotubes based on organic–inorganic hybrid approach, Prog. Org. Coat. 76 (2013) 1251–1257. doi:10.1016/j.porgcoat.2013.03.022.

[3] M. Kozako, H. Nakatsu, H. Toda, S. Yamada, K. Yoshinaga, M. Hikita, et al., Basic Investigation of epoxy resin coatings with dispersed carbon nanotubes, Electron. Comm. Jpn. 97 (2014) 24–32. doi:10.1002/ecj.11555.

[4] S.M. Yuen, C.C.M. Ma, Y.Y. Lin, H.C. Kuan, Preparation, morphology and properties of acid and amine modified multiwalled carbon nanotube/polyimide composite, Compos. Sci. Technol. 67 (2007) 2564–2573. doi:10.1016/j.compscitech.2006.12.006.

[5] Y.G. Jeong, J.E. An, Effects of mixed carbon filler composition on electric heating behavior of thermally-cured epoxy-based composite films, Compos. Part A. 56 (2014) 1–7. doi:10.1016/j.compositesa.2013.09.003.

[6] Y. Show, T. Nakashima, Y. Fukami, Anticorrosion coating of carbon nanotube/polytetrafluoroethylene composite film on the stainless steel bipolar plate for proton

exchange membrane fuel cells, J. Nanomater. 2013 (2013) e378752. doi:10.1155/2013/378752.
[7] Y.C. Huang, J.H. Lin, I.H. Tseng, A.Y. Lo, T.Y. Lo, H.P. Yu, et al., An in situ fabrication process for highly electrical conductive polyimide/MWCNT composite films using 2,6-diaminoanthraquinone, Compos. Sci. Technol. 87 (2013) 174–181. doi:10.1016/j.compscitech.2013.08.008.
[8] H. Kobayashi, M. Shioya, T. Tanaka, T. Irisawa, Synchrotron radiation small-angle X-ray scattering study on fracture process of carbon nanotube/poly(ethylene terephthalate) composite films, Compos. Sci. Technol. 67 (2007) 3209–3218. doi:10.1016/j.compscitech.2007.04.005.
[9] A. Gergely, Z. Pászti, J. Mihály, E. Drotár, T. Török, Galvanic function of zinc-rich coatings facilitated by percolating structure of the carbon nanotubes. Part II: Protection properties and mechanism of the hybrid coatings, Prog. Org. Coat. 77 (2014) 412–424. doi:10.1016/j.porgcoat.2013.11.004.
[10] B.H. Ryu, A.J. Barthel, H.J. Kim, H.D. Lee, O.V. Penkov, S.H. Kim, et al., Tribological properties of carbon nanotube–polyethylene oxide composite coatings, Compos. Sci. Technol. 101 (2014) 102–109. doi:10.1016/j.compscitech.2014.07.007.
[11] L.H. Esposito, J.A. Ramos, G. Kortaberria, Dispersion of carbon nanotubes in nanostructured epoxy systems for coating application, Prog. Org. Coat. 77 (2014) 1452–1458. doi:10.1016/j.porgcoat.2014.05.001.
[12] J.J. Hernández, M.C. García-Gutiérrez, D.R. Rueda, T.A. Ezquerra, R.J. Davies, Influence of single wall carbon nanotubes and thermal treatment on the morphology of polymer thin films, Compos. Sci. Technol. 72 (2012) 421–427. doi:10.1016/j.compscitech.2011.12.003.
[13] K. Kowalczyk, S. Kugler, T. Spychaj, Antistatic polyurethane coats with hybrid carbon nanofillers, Polimery. 59 (2014) 650–655. doi:10.14314/polimery.2014.650.
[14] S. Kugler, K. Kowalczyk, T. Spychaj, Hybrid carbon nanotubes/graphene modified acrylic coats, Prog. Org. Coat. 85 (2015) 1–7. doi:10.1016/j.porgcoat.2015.02.019.
[15] L. Liu, J.C. Grunlan, Clay assisted dispersion of carbon nanotubes in conductive epoxy nanocomposites, Adv. Funct. Mater. 17 (2007) 2343–2348. doi:10.1002/adfm.200600785.
[16] Y. Li, H. Shimizu, Conductive PVDF/PA6/CNTs nanocomposites fabricated by dual formation of cocontinuous and nanodispersion structures, Macromolecules 41 (2008) 5339–5344. doi:10.1021/ma8006834.
[17] C.R. Yu, D.M. Wu, Y. Liu, H. Qiao, Z.Z. Yu, A. Dasari, et al., Electrical and dielectric properties of polypropylene nanocomposites based on carbon nanotubes and barium titanate nanoparticles, Compos. Sci. Technol. 71 (2011) 1706–1712. doi:10.1016/j.compscitech.2011.07.022.
[18] O. Meincke, D. Kaempfer, H. Weickmann, C. Friedrich, M. Vathauer, H. Warth, Mechanical properties and electrical conductivity of carbon-nanotube filled polyamide-6 and its blends with acrylonitrile/butadiene/styrene, Polymer. 45 (2004) 739–748. doi:10.1016/j.polymer.2003.12.013.
[19] A. Dasari, Z.Z. Yu, Y.W. Mai, Electrically conductive and super-tough polyamide-based nanocomposites, Polymer. 50 (2009) 4112–4121. doi:10.1016/j.polymer.2009.06.026.
[20] Y. Sun, H.D. Bao, Z.X. Guo, J. Yu, Modeling of the electrical percolation of mixed carbon fillers in polymer-based composites, Macromolecules 42 (2009) 459–463. doi:10.1021/ma8023188.
[21] H.D. Bao, Z.X. Guo, J. Yu, Effect of electrically inert particulate filler on electrical resistivity of polymer/multi-walled carbon nanotube composites, Polymer. 49 (2008) 3826–3831. doi:10.1016/j.polymer.2008.06.024.

[22] Y. Sun, M.Y. Jia, Z.X. Guo, J. Yu, S. Nagai, Effect of styrene–acrylonitrile on the electrical resistivity of polycarbonate/multiwalled carbon nanotube composites, J. Appl. Polym. Sci. 120 (2011) 3224–3232. doi:10.1002/app.33361.
[23] H. Wang, X. Zhang, Y. Zhu, Z. Song, J. Qiao, Reducing resistivity of polyamide-6/multi-walled carbon nanotube composites by adding ultra-fine rubber particles on account of non-volume exclusion effect, Mater. Lett. 65 (2011) 2055–2058. doi:10.1016/j.matlet.2011.03.108.
[24] H. Palza, B. Reznik, M. Wilhelm, O. Arias, A. Vargas, Electrical, thermal, and mechanical characterization of poly(propylene)/carbon nanotube/clay hybrid composite materials, Macromol. Mater. Eng. 297 (2012) 474–480. doi:10.1002/mame.201100249.
[25] S.P. Bao, G.D. Liang, S.C. Tjong, Positive temperature coefficient effect of polypropylene/carbon nanotube/montmorillonite hybrid nanocomposites, IEEE T. Nanotechnol. 8 (2009) 729–736. doi:10.1109/TNANO.2009.2023650.
[26] M. Feng, X. Huang, Z. Pu, X. Liu, Dielectric and mechanical properties of three-component Al_2O_3/MWCNTs/polyarylene ether nitrile micro-nanocomposite, J. Mater. Sci.: Mater. Electron. 25 (2014) 1393–1399. doi:10.1007/s10854-014-1740-6.
[27] M. Berkei, Conductive coatings using carbon nanotubes, CHEManager Europe. 7-8 (2011) 10. http://www.chemanager-online.com/en/magazine/chemanager-europe-7-82011.
[28] J. Sumfleth, L.A.S. de A. Prado, S. Richau, M. Sriyai, K. Schulte, Enhanced dispersion of MWCNTs and synergistic properties in multiphase epoxy nanocomposites by incorporation of inorganic nanoparticles, Sol. St. Phen. 151 (2009) 176–180. doi:10.4028/www.scientific.net/SSP.151.176.
[29] J. Sumfleth, L.A.S. de Almeida Prado, M. Sriyai, K. Schulte, Titania-doped multi-walled carbon nanotubes epoxy composites: Enhanced dispersion and synergistic effects in multiphase nanocomposites, Polymer 49 (2008) 5105–5112. doi:10.1016/j.polymer.2008.09.016.
[30] L.C. Tang, Y.J. Wan, K. Peng, Y.B. Pei, L.B. Wu, L.M. Chen, et al., Fracture toughness and electrical conductivity of epoxy composites filled with carbon nanotubes and spherical particles, Compos. Part A. 45 (2013) 95–101. doi:10.1016/j.compositesa.2012.09.012.
[31] T. Spychaj, S. Spychaj, Water-thinnable paints and adhesives, WNT, Warsaw, 1996.
[32] S. Bhargava, R.D. Lewis, M. Kubota, X. Li, S.G. Advani, J.M. Deitzel, et al., Adhesion study of high reflectivity water-based coatings, Int. J. Adhes. Adhes. 40 (2013) 120–128. doi:10.1016/j.ijadhadh.2012.07.002.
[33] K. Kowalczyk, K. Łuczka, B. Grzmil, Preparation and characterization of anticorrosion polyurethane paints and coatings based on novel Zn-free phosphates, J. Coat. Technol. Res. (2014) 1–13. doi:10.1007/s11998-014-9612-9.
[34] N.W. Khun, B.C.R. Troconis, G.S. Frankel, Effects of carbon nanotube content on adhesion strength and wear and corrosion resistance of epoxy composite coatings on AA2024-T3, Prog. Org. Coat. 77 (2014) 72–80. doi:10.1016/j.porgcoat.2013.08.003.
[35] A.K. Keshri, D. Lahiri, A. Agarwal, Carbon nanotubes improve the adhesion strength of a ceramic splat to the steel substrate, Carbon. 49 (2011) 4340–4347. doi:10.1016/j.carbon.2011.06.010.
[36] J. Grunlan, Y.-S. Kim, S. Ziaee, X. Wei, B. Abdel-Magid, K. Tao, Thermal and mechanical behavior of carbon-nanotube-filled latex, Macromol. Mater. Eng. 291 (2006) 1035-1043. doi:10.1002/mame.200600191

[37] S. Ud Din Khan, M. Arora, C. Puri, M.A. Wahab, P. Saini, Synthesis and characterization of acrylic resin/activated carbon composites, Indian J. Pure Appl. Phys. 52 (2014) 251–254.

[38] P. Saini, M. Arora, Microwave absorption and EMI shielding behavior of nanocomposites based on intrinsically conducting polymers, graphene and carbon nanotubes, in: New polymers for special applications, Intech Open Science, 2012. doi:10.5772/48779.
[39] S. Pande, B.P. Singh, R.B. Mathur, T.L. Dhami, P. Saini, S.K. Dhawan, Improved electromagnetic interference shielding properties of MWCNT–PMMA composites using layered structures, Nanoscale Res. Lett. 4 (2009) 327. doi:10.1007/s11671-008-9246-x.
[40] P. Saini, V. Choudhary, Enhanced electromagnetic interference shielding effectiveness of polyaniline functionalized carbon nanotubes filled polystyrene composites, J. Nanopart. Res. 15 (2013) 1–7. doi:10.1007/s11051-012-1415-2.

FIGURES

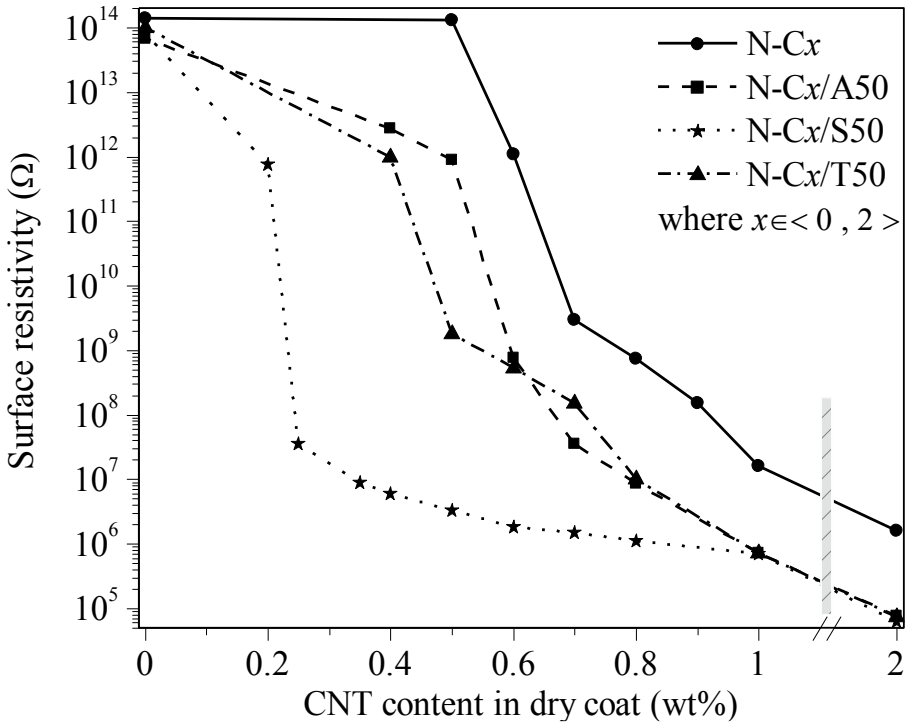

Fig. 1. Electrical surface resistivity of acrylic coatings with carbon nanotubes (CNT) and 50 wt.% of dielectric inorganic nanoparticles.

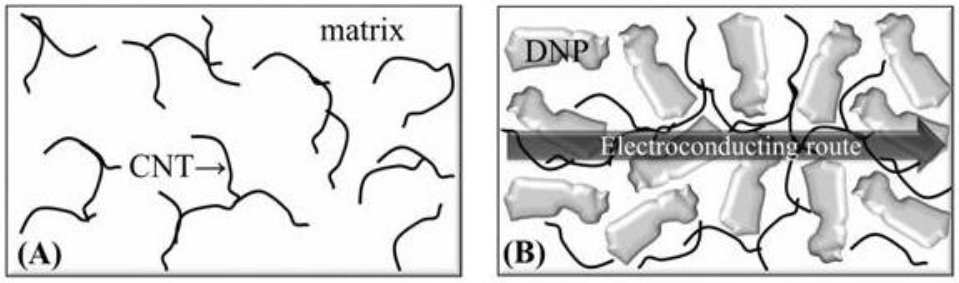

Fig. 2. Scheme of CNT-based nanocomposite (A) without dielectric inorganic nanoparticles (DNP) and (B) with DNP added replacing a part of polymeric matrix.

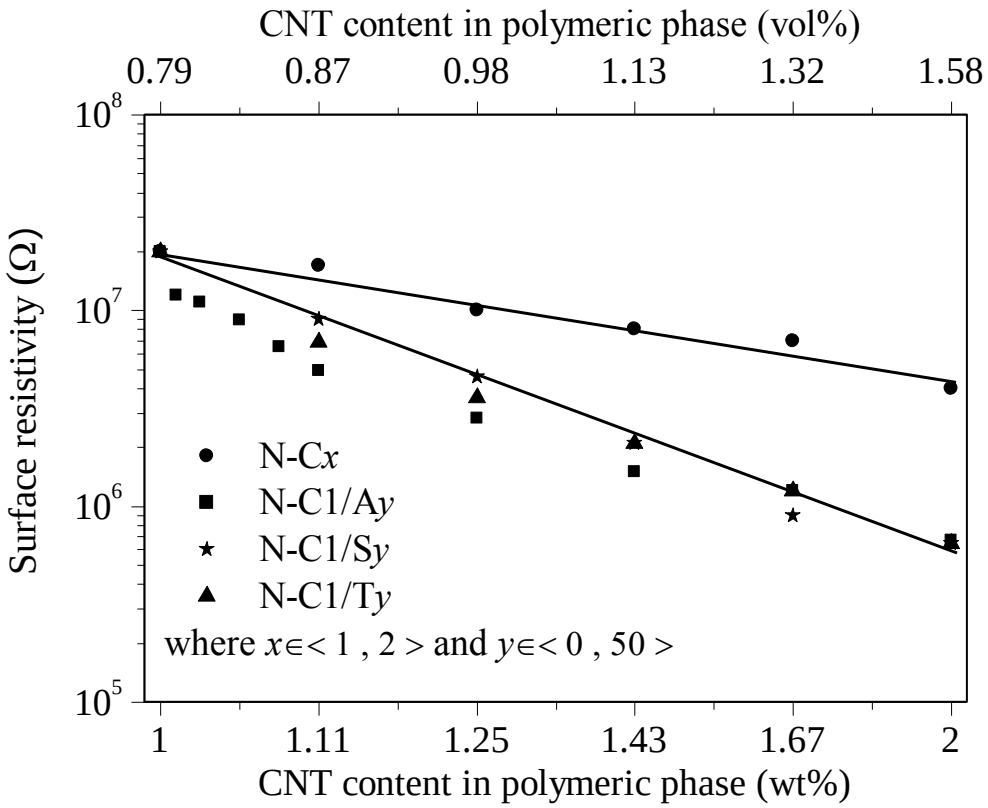

Fig. 3. Electrical surface resistivity of acrylic coatings with various CNT content in the polymeric phase (samples with and without dielectric inorganic nanoparticles)

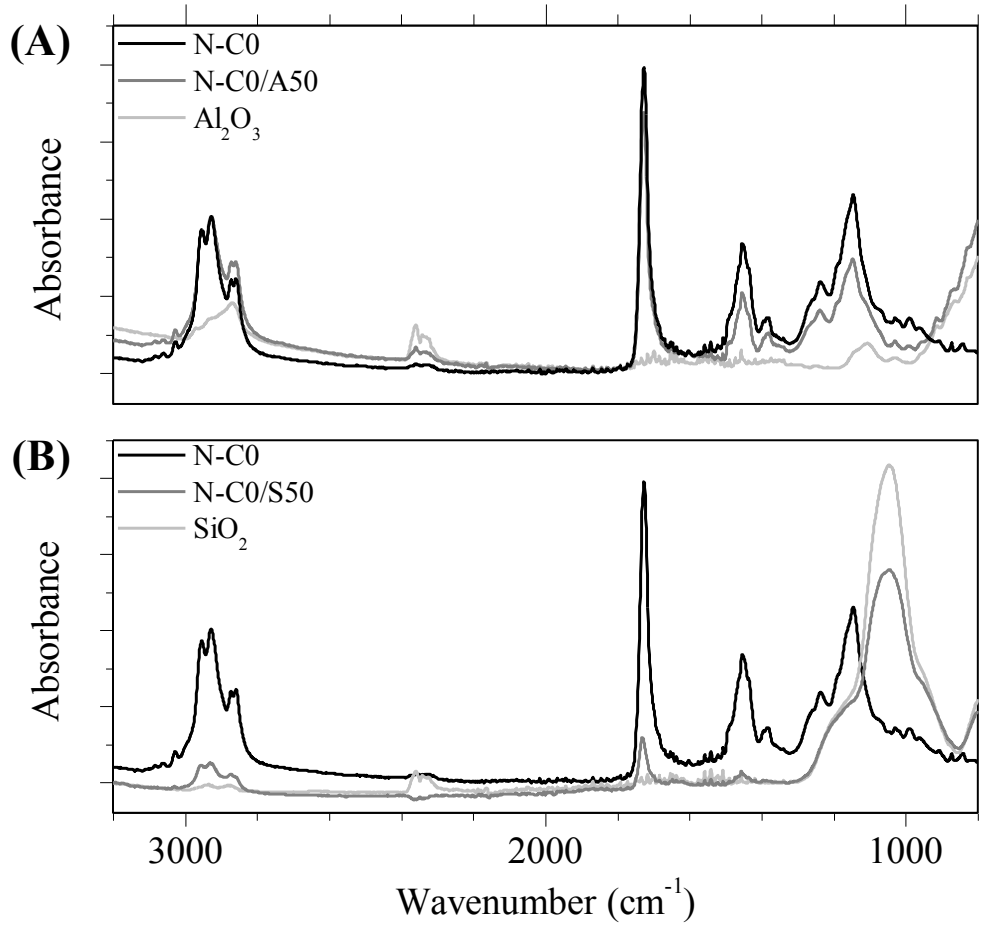

Fig. 4. FT-IR spectra of (A) alumina and coating containing alumina and (B) silica and a coating containing silica.

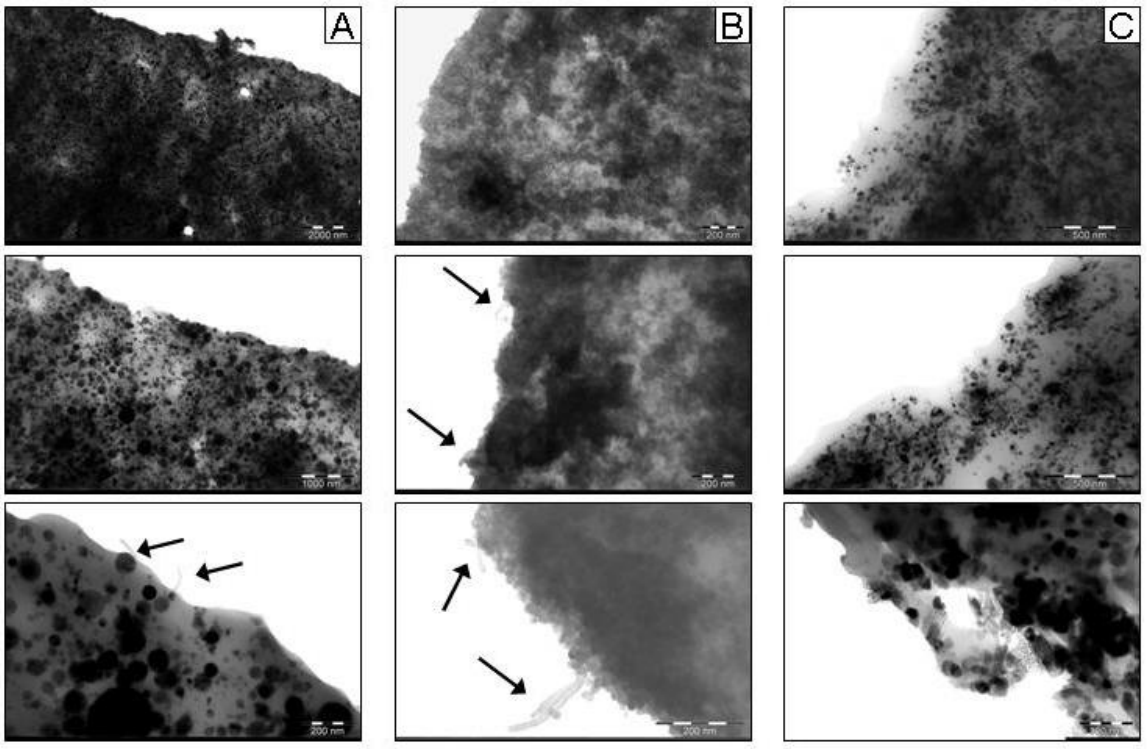

Fig. 5. TEM images of acrylic coatings with 1 wt.% of CNT and 50 wt.% of (A) alumina, (B) silica or (C) titania (arrows show CNT on the surface).

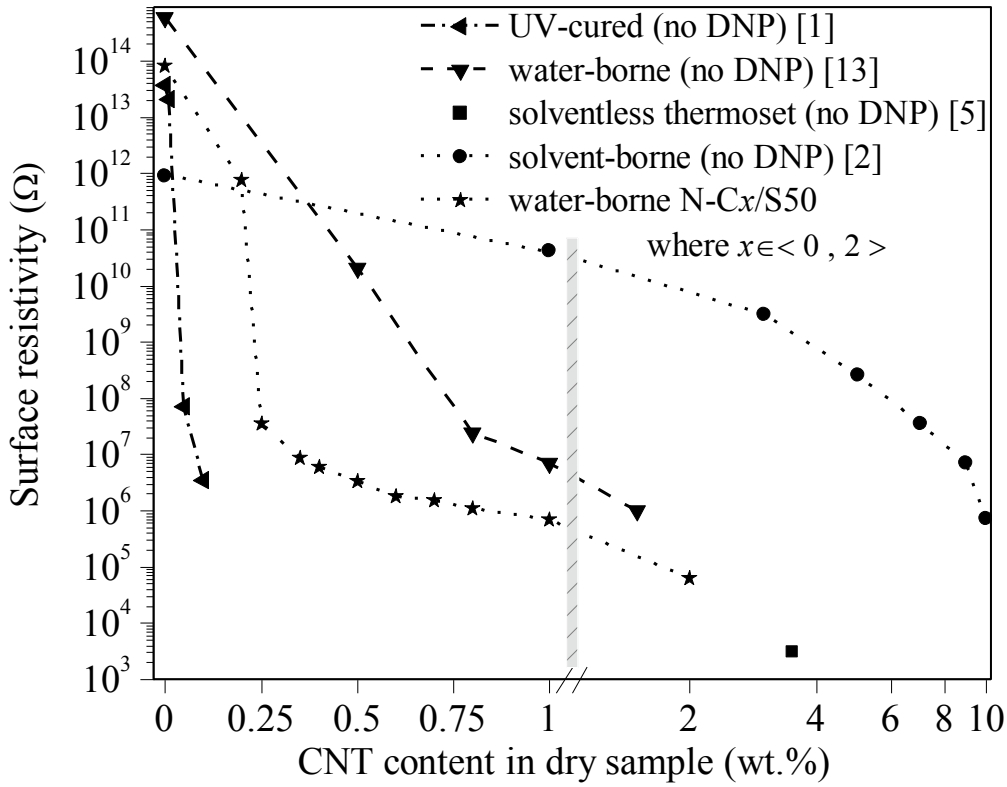

Fig. 6. Electrical surface resistivity of various coating systems containing CNT.

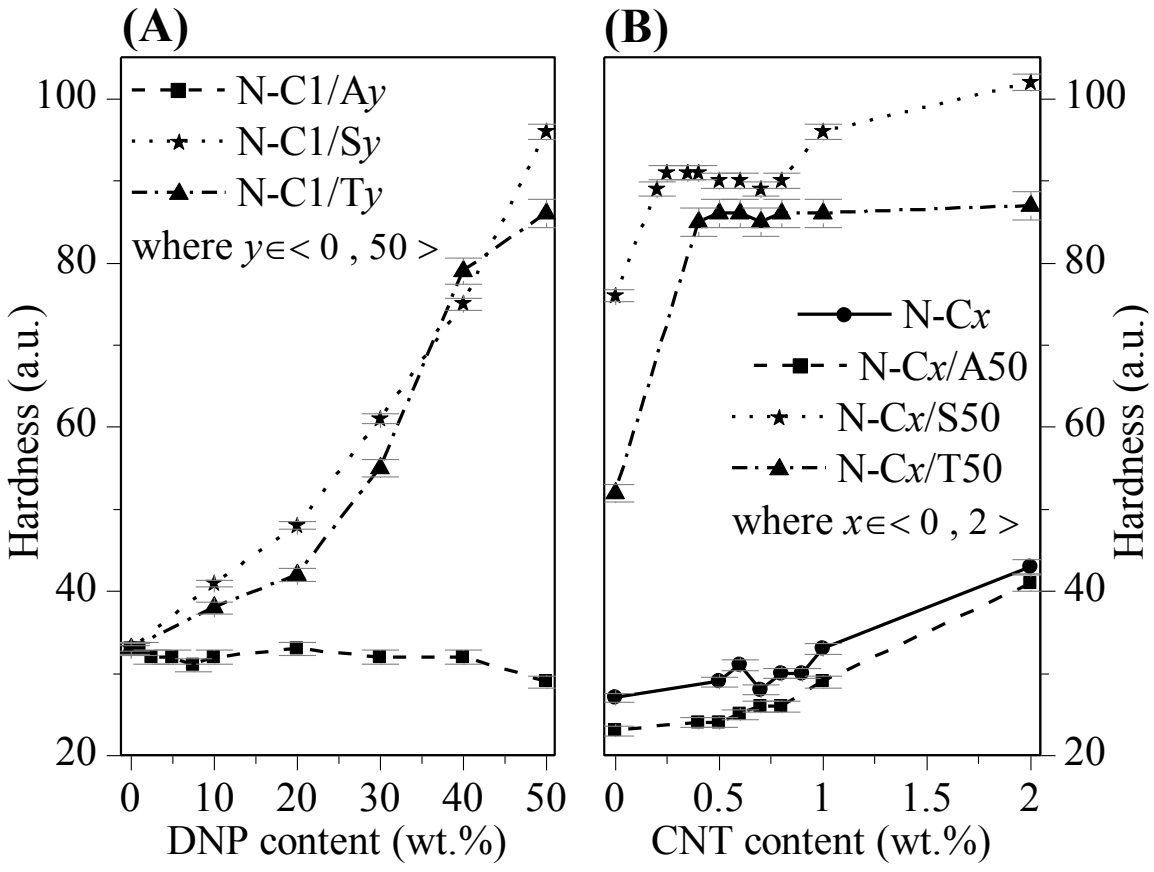

Fig. 7. Hardness of acrylic coatings in relation to (A) DNP content in a dry sample (1 wt.% of CNT) and (B) CNT content in a dry sample.

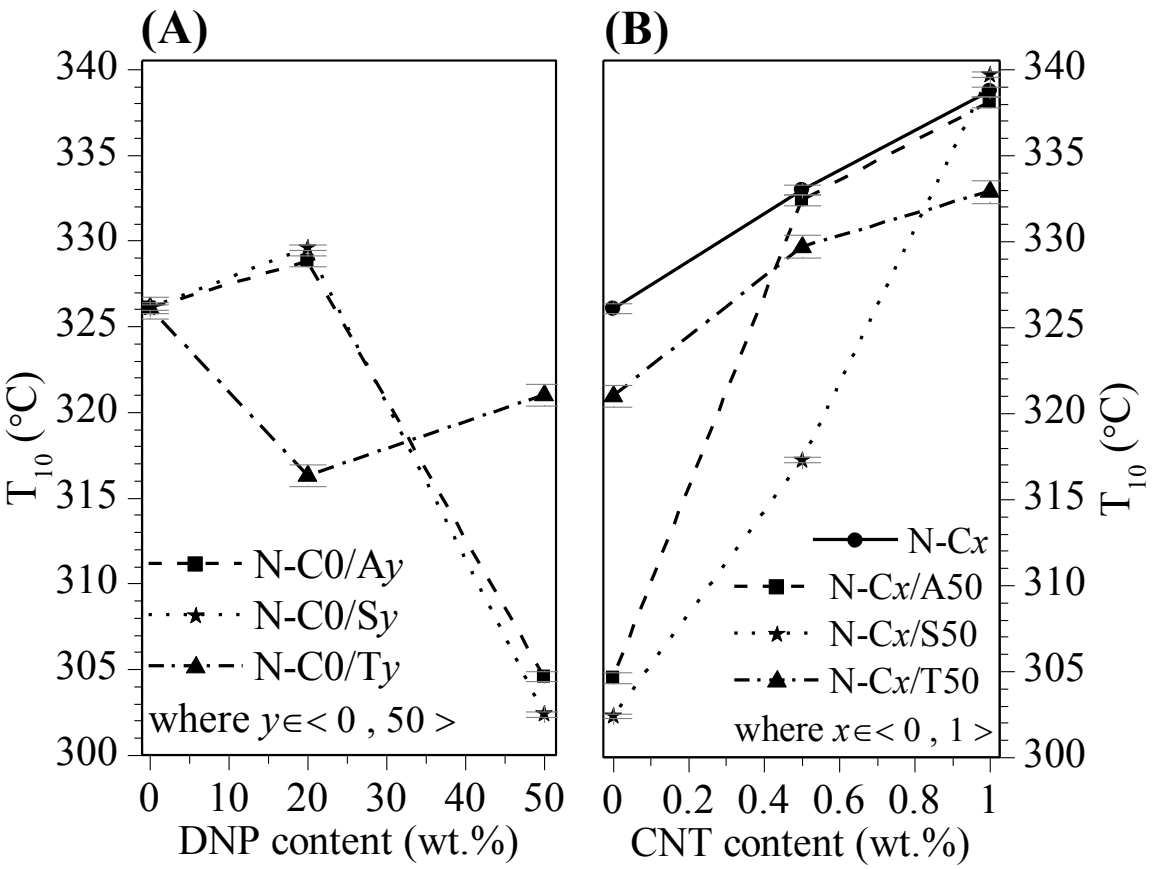

Fig. 8. Temperature at 10 % mass loss (T_{10}) of acrylic coatings in relation to (A) DNP content in a dry sample (no CNT) and (B) CNT content in a dry sample (50 wt.% of DNP).

TABLES

Table 1. Properties of acrylic coatings with carbon nanotubes and inorganic oxide nanoparticles.

Sample acronym	CNT content [a]	DNP		Surface resistivity (Ω)	Transparency [b] (%)	Gloss (G.U.)	Adhesion (°) [c]	T_g [d] (°C)	
		Type	Content [a]					DSC	DMA
N-C0	0	—	0	$1.4 \cdot 10^{14}$	87	142	0	-10.3 / 51.0	-15.8
N-C0.5	0.5			$1.3 \cdot 10^{14}$	36	82	0	-10.0 / 51.0	-14.0
N-C1	1			$1.6 \cdot 10^{7}$	14	80	0	-10.4 / 51.3	-14.8
N-C0/S20	0	SiO_2	20	$1.0 \cdot 10^{14}$	85	88	0	-10.3 / 51.4	-14.9
N-C0/S50	0		50	$8.1 \cdot 10^{13}$	84	65	3	-10.4 / 50.2	-12.4
N-C0.25/S50	0.25			$3.6 \cdot 10^{7}$	70	62	2	-10.0 / 51.0	-13.8
N-C0.5/S50	0.5			$3.3 \cdot 10^{6}$	45	57	2	-10.5 / 51.0	-14.5
N-C1/S50	1			$7.0 \cdot 10^{5}$	22	48	2	-10.4 / 51.1	-17.4
N-C0/A20	0	Al_2O_3	20	$1.0 \cdot 10^{14}$	76	103	2	-11.2 / 48.4	-15.5
N-C0/A50	0		50	$6.8 \cdot 10^{13}$	71	111	2	-11.6 / 47.7	-16.8
N-C0.5/A50	0.5			$8.9 \cdot 10^{11}$	35	87	1	-11.9 / 47.0	-13.5
N-C1/A50	1			$7.3 \cdot 10^{5}$	15	76	1	-11.4 / 47.0	-15.5
N-C0/T20	0	TiO_2	20	$1.2 \cdot 10^{14}$	5	16	1	-12.8 / 51.3	-15.5
N-C0/T50	0		50	$1.0 \cdot 10^{14}$	3	1	1	-12.8 / 52.7	-16.8
N-C0.5/T50	0.5			$1.8 \cdot 10^{9}$	0.7	0.5	0	-12.0 / 50.4	-13.5
N-C1/T50	1			$7.3 \cdot 10^{5}$	0.6	0.3	0	-12.8 / 50.6	-15.5

a – wt.%; b – at 550 nm; c – rating scale 0-5 (0 – the best, 5 – the worst); d – glass transition temperature(s) determined by DSC and DMA techniques;

SUPPLEMENTS

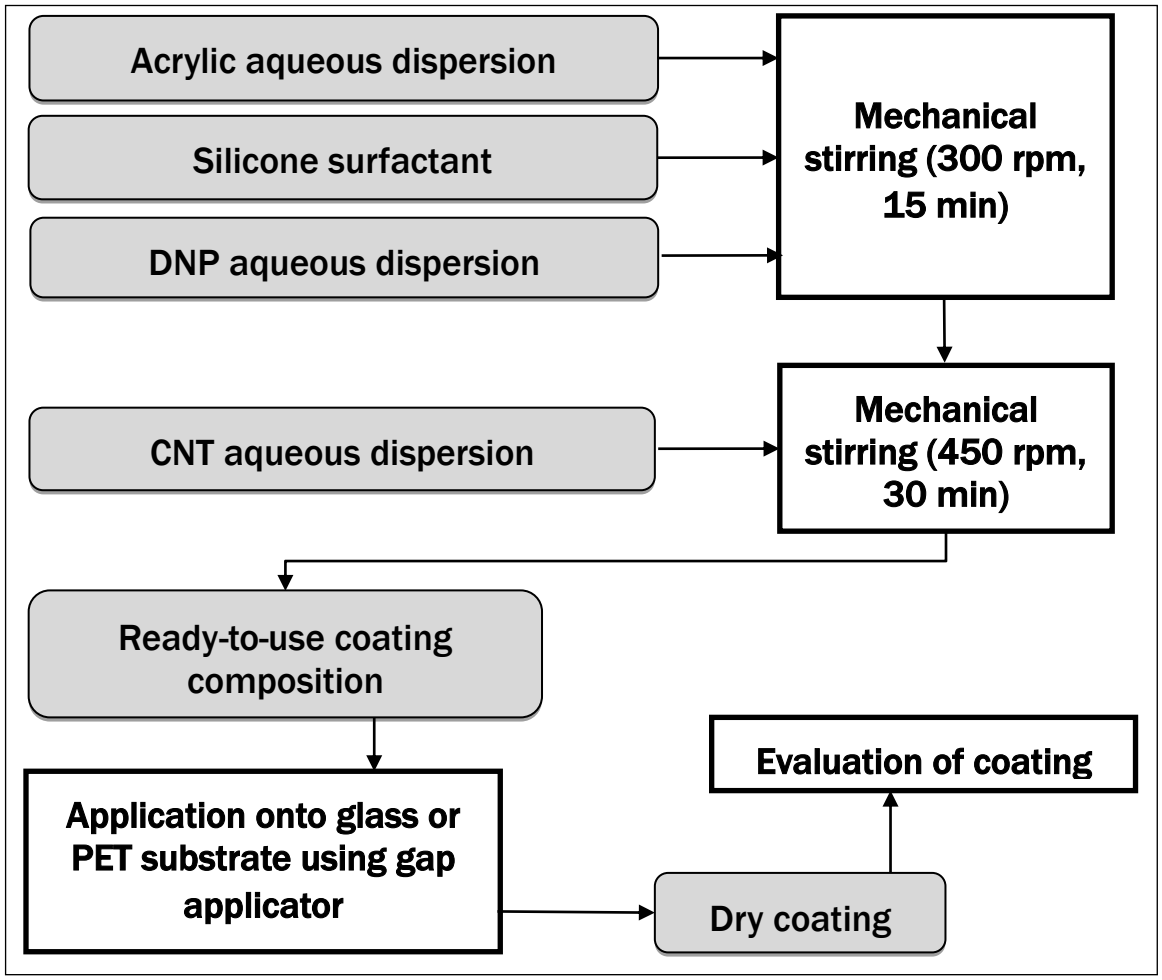

Supplement 1. Preparation scheme for acrylic coatings containing carbon nanotubes (CNT) and dielectric inorganic oxide nanoparticles (DNP).

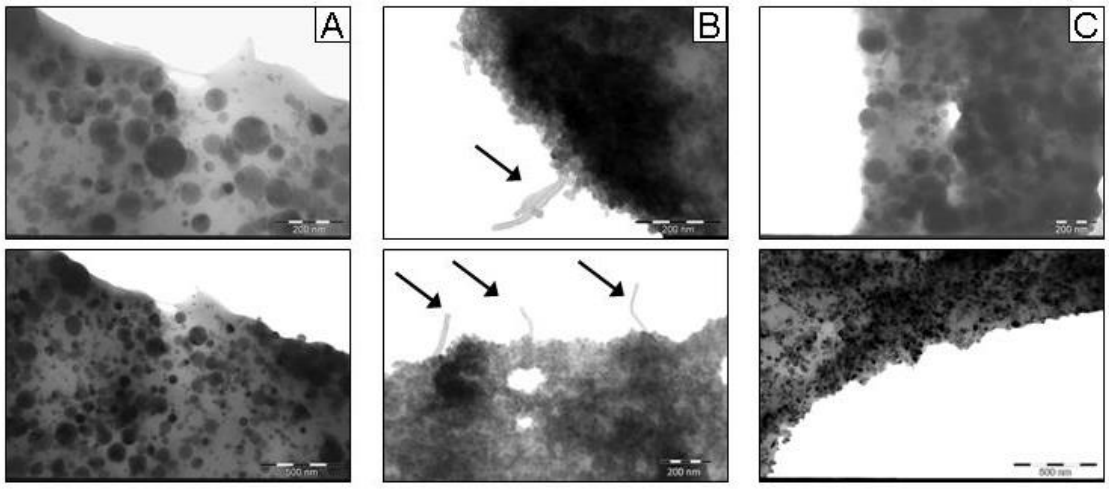

Supplement 2. TEM images of acrylic coatings with 1 wt.% of CNT and 50 wt.% of (A) alumina, (B) silica or (C) titania (arrows show CNT on the surface).